Modeling Analysis of Corrosion Behavior of Carbon Steel in CO_2 Loaded Amine Solutions

Abdelbaki Benamor and Mohammed Jaber Al-Marri

***Abstract*—A mathematical model simulating the corrosion behavior of carbon steel in aqueous amine-CO_2 environment was developed and used to analyze the corrosion phenomena in CO_2 loaded amine solutions. A mechanistic corrosion model is applied to identify the most important agents responsible for the corrosion behavior of carbon steel. The model incorporates an equilibrium model based on an activity coefficient approach according to Debye-Huckel theory and mixed potential theory to simulate the concentration of chemical species and polarization behavior taking place at a metal-solution interface in a DEA-CO_2-H_2O system. Simulated anodic and cathodic polarization curves were established on the basis of the calculated species concentration to represent the hypothetical oxidation and reduction behavior which were compared to the experimental curves to come out with the best fit revealing the most important corroding agents.**

***Index Terms*—Corrosion model, diethanolamine, carbon dioxide, equilibrium model, mixed potential theory, polarization curve.**

I. Introduction

Concentration of carbon dioxide (CO_2) in the atmosphere is known to have a direct linkage to global climate changes. One method to reduce the emission of this greenhouse gas is the absorption process. The CO_2 absorption process using aqueous amine solutions is a well-established separation technique in chemical industries such as natural gas sweetening, coal gasification and manufacturing of ammonia. Aqueous amine solution removes acidic gases mainly such as CO_2 and mercaptans by forming a salt in order to achieve the required product quality and to minimize operational difficulties, which may occur in downstream processes [1].

Severe corrosion essentially results in substantial expenditure for amine treating plants. Other than maintenance-related expenses due to corrosion, safety of plant personnel is also an issue considering an incident caused by severe corrosion occurred on 23 July 1984 in a refinery owned by the Union Oil Co. of California.

Amine itself is not corrosive, but the CO_2 absorption process using aqueous amine solutions has long encountered corrosion problems despite the fact that it has been used in industries for over half a century [2]. In fact, studies revealed that dissolved CO_2 in aqueous solutions could lead to severe corrosion damage to transportation and process equipment of crude oil and natural gas [3], [4]. Plant areas that are susceptible to corrosion are the bottom of the absorbers, lean-rich exchanger, reboiler bundles, regenerator units and the overhead condenser where the acid gas loading and temperatures are relatively high [5]. The most widely used single amines for the absorption process include monoethanolamine (MEA), 2-amino-methyl-1-propanol (AMP), diethanolamine (DEA) and methyldiethanolamine (MDEA). These chemical solvents enhance gas absorption capacity and act to improve selectivity. MEA attracts the greatest interest because it is very reactive and able to yield a high volume of acid gas removal at a fast rate [6]. The use of mixed amines as solvent also improves the performance of specific gas stream composition [7]. Among others, Pauline *et al*. [8] used electrochemical techniques to investigate the influence of amines on the corrosion behavior in CO_2 capture plants. The same approach was used by Zhao *et al.* [9] to study the corrosion phenomena in CO_2 chemical absorption process using mixtures of MDEA and Piperazine solution, the effect of flue gas composition impurities on carbon steel corrosion was investigated by Wattanaphan *et al*. [10] for MEA based CO_2 capture process.

There have been many studies conducted on electrochemical and corrosion behaviour of metal and alloys in organic solvents. According to Richard [11], four steps must be present for corrosion to occur namely oxidation-anodic half-cell reaction, reduction-cathodic half-cell reaction, ionic transport for conductive medium and electron transport between the anode and cathode sites. Consequently, eliminating one of these processes can be very useful as a first measure to avoid corrosion.

Industrial gas absorption process requires fast absorption rates and high solvent capacity that is easily regenerated and volume make-up is minimized [7]. The shortcomings caused by the nature of solvent and the type of solute-solvent interactions have been studied extensively. However, there exists a lack of studies in determining the main agents responsible for the corrosion behaviour in amine-CO_2 solutions. Corrosion mechanism in aqueous amine-CO_2 solutions is usually described without proper verification by a number of oxidation reactions represented by H^+ and HCO_3^- [12]. Therefore, it is necessary to identify the oxidizing agents responsible for the corrosion in amine-CO_2 systems.

The use of prediction model on CO_2 corrosion behaviour was recommended instead of time consuming experiments [13]. Several numerical models provided some insight into the underlying physicochemical processes [14], [15]. However, a more recent model based on mechanistic descriptions of CO_2 corrosion mechanisms could be created to cover various types of corrosion by small modifications of species and corresponding electrochemical reactions implemented onto it [16].

Manuscript received November 30, 2013; revised January 8, 2014.

The authors are with Gas processing Center, Faculty of Engineering, Qatar University, P. O. Box 2713, Doha, Qatar (e-mail: benamor.abdelbaki@qu.edu.qa, m.almarri@qu.edu.qa).

DOI: 10.7763/IJCEA.2014.V5.408

The ultimate goal of this research is to identify the oxidizing agents responsible for corrosion in the H_2O-DEA-CO_2 system at a fixed temperature and various CO_2 loading. From this determination, we could identify and control the parameters in the system that plays a significant role in the corrosion process.

II. Model Development

In aqueous DEA-CO_2 environment, two types of reactions coexist at the metal-solution interface; namely chemical and electrochemical reactions. There are seven chemical reactions and four electro-chemical reactions as presented in Table I. The first five chemical reactions involve typical CO_2 absorption reactions in an aqueous amine solution while the other two are reactions which form corrosion products in a de-aerated aqueous CO_2 environment.

TABLE I: Reactions Taking Place at the Metal-Solution Interface

NO	Description	Reaction	
1	Dissociation of protonated-amine	$DEAH_2^+ + H_2O \overset{K_1}{\leftrightarrow} H_3O^+ + DEAH$	Chemical reactions
2	Carbamate reversion	$DEACOO^- + H_2O \overset{K_2}{\leftrightarrow} DEAH + HCO_3^-$	
3	Hydrolysis of carbon dioxide	$2H_2O + CO_2 \overset{K_3}{\leftrightarrow} H_3O^+ + CO_3^-$	
4	Dissociation of water	$2H_2O \overset{K_4}{\leftrightarrow} H_3O^+ + OH^-$	
5	Dissociation of bicarbonate ion	$H_2O + HCO_3^- \overset{K_5}{\leftrightarrow} H_3O^+ + CO_3^{2-}$	
6	Formation of ferrous hydroxide	$Fe^{2+} + 2OH^- \overset{K_6}{\leftrightarrow} Fe(OH)_2$	
7	Formation of ferrous carbonate	$Fe^{2+} + CO_3{}^{2-} \overset{K_7}{\leftrightarrow} FeCO_3$	
8	Iron dissolution	$Fe \overset{K_8}{\leftrightarrow} Fe^{2+} + 2e^-$	Electro-chemical reactions
9	Reduction of hydronium ion	$2H_3O^+ + 2e^- \overset{K_9}{\leftrightarrow} 2H_2O + H_2$	
10	Reduction of bicarbonate ion	$2HCO_3{}^- + 2e^- \overset{K_{10}}{\leftrightarrow} 2CO_3{}^{2-} + H_2$	
11	Reduction of undissociated water	$2H_2O + 2e^- \overset{K_{11}}{\leftrightarrow} à2OH^- + H_2$	

III. Methodology

The development of the corrosion model comprises two major steps: determination of species concentration at the metal-solution interface using the mathematical model and establishment of polarization curves based on the calculated species concentrations.

A. Surface Concentration of Chemical Species

There are twelve chemical species at the metal-solution interface. All chemical species were considered as unknown except that of water. As a result, 11 equations as shown in Table II were required to solve 11 independent variables.
where *r* denotes any reduction reaction in Equation (E11).

The associated equilibrium constants K_i were written in terms of activity coefficients γ_i . Their temperature dependency is given by:

$$\ln K_i = \frac{a_i}{T} + b_i \ln T + c_i T + d \tag{12}$$

The activity coefficients are given by:

$$\ln \gamma_i = -\frac{2.303 A Z_i{}^2 \sqrt{I}}{1 + B\sqrt{I}} + 2\sum \beta_{i,j} m_j \tag{13}$$

where Z_i and m_j are the electrical charges and concentrations of the corresponding species respectively. The term I represents the ionic strength of the solution.

The value of A was taken from the literature [17] and B equals to 1.2, as was suggested by Pitzer [18], [19]. $\beta_{i,j}$ are the interaction parameters between the different ionic and molecular species in the system excluding interactions between solutes and solvent and are represented in the following form:

$$\beta_{i,j} = a_{i,j} + b_{i,j} T \tag{14}$$

where $a_{i,j}$ and $b_{i,j}$ are taken from literature [20]. The ionic strength, I, of the solution was calculated by:

$$I = \frac{1}{2}\sum m_j Z_j{}^2 \tag{15}$$

Equations (E6) and (E7) represent the equilibrium formation of corrosion products. Equilibrium constants $K_{Fe(OH)_2}$ and K_{FeCO_3} were derived from a relationship between standard Gibbs free energy (ΔG°) and the equilibrium constant (K) [21].

TABLE II: EQUATIONS USED IN THE CORROSION MODEL

N^O	Description	Equation
E1	Equilibrium dissociation of protonated amine	$K_1=\frac{[DEAH].[H_3O^+]}{[DEAH_2^+].[H_2O]}.\frac{(\gamma_{DEAH}.\gamma_{H_3O^+})}{(\gamma_{DEAH_2^+}.\gamma_{H_2O})}$
E2	Equilibrium carbamate reversion	$K_2=\frac{[DEAH].[HCO_3^-]}{[DEACOO^-].[H_2O]}.\frac{(\gamma_{DEAH}.\gamma_{HCO_3^-})}{(\gamma_{DEACOO^-}.\gamma_{H_2O})}$
E3	Equilibrium hydrolysis of carbon dioxide	$K_3=\frac{[H_3O^+].[HCO_3^-]}{[CO_2].[H_2O]^2}.\frac{(\gamma_{H_3O^+}.\gamma_{HCO_3^-})}{(\gamma_{CO_2}.\gamma_{H_2O}^2)}$
E4	Equilibrium dissociation of water	$K_4=\frac{[H_3O^+].[OH^-]}{[H_2O]^2}.\frac{(\gamma_{H_3O^+}.\gamma_{OH^-})}{(\gamma_{H_2O})^2}$
E5	Equilibrium dissociation of bicarbonate ion	$K_5=\frac{[H_3O^+].[CO_3^{2-}]}{[HCO_3^-].[H_2O]}\frac{(\gamma_{H_3O^+}.\gamma_{CO_3^{2-}})}{(\gamma_{HCO_3^-}.\gamma_{H_2O})}$
E6	Equilibrium formation of ferrous hydroxide	$K_6=\frac{[Fe(OH)_2]}{[Fe^{2+}].[OH^-]^2}\frac{\gamma_{Fe(OH)_2}}{(\gamma_{Fe^{2+}}\gamma_{OH^-}^2)}$
E7	Equilibrium formation of ferrous carbonate	$K_7=\frac{[FeCO_3]}{[Fe^{2+}].[CO_3^{2-}]}.\frac{\gamma_{FeCO_3}}{(\gamma_{Fe^{2+}}.\gamma_{CO_3^{2-}})}$
E8	Charge balance	$\left[DEACOO^-\right]+\left[OH^-\right]+\left[HCO_3^-\right]+2\left[CO_3^{2-}\right]-\left[DEAH_2^+\right]-\left[H_3O^+\right]-2\left[Fe^{2+}\right]=0$
E9	Mass balance for amine	$\left[DEAH\right]_{Tot}-\left[DEACOO^-\right]-\left[DEAH\right]-\left[DEAH_2^+\right]=0$
E10	Mass balance for carbon	$\alpha_{CO_2}\left[DEAH\right]_{Tot}-\left[DEACOO^-\right]-\left[HCO_3^-\right]-\left[CO_3^{2-}\right]-\left[CO_2\right]-\left[FeCO_3\right]=0$
E11	Mixed Potential	$i_{0,Fe^{2+}}\times10^{(E-E_{rev,Fe^{2+}})/\beta_{Fe^{2+}}}=\sum_r i_{0,r}\times10^{(E-E_{rev,r})/\beta_r}$

$$\Delta G^{\circ}=-RT\ \ln K \tag{16}$$

Equation (E11) was derived from mixed potential theory [22]. At equilibrium, the rate of oxidation must be equal to that of reduction.

$$\sum i_{oxidation}=\sum i_{reduction} \tag{17}$$

Since iron dissolution is the only oxidation reaction, the oxidation rate is expressed as:

$$\sum i_{oxidation}=i_{Fe/Fe^{2+}} \tag{18}$$

The iron dissolution is said to be under activation (charge transfer) control because of the unlimited supply of Fe. In this case, the relationship between current density (i) and potential (E) is defined as:

$$i_{Fe/Fe^{2+}}=i_{0,Fe/Fe^{2+}}\times10^{\frac{(E-E_{rev,Fe/Fe^{2+}})}{\beta_{Fe/Fe^{2+}}}} \tag{19}$$

The potential reduction reactions participating in the corrosion process are reaction (9-11), in which H_3O^+, HCO_3^- and H_2O serve as oxidizing agents. By considering the three species are actual oxidizing agents in H_2O-DEA-CO_2 environment, the total reduction rate will be:

$$\sum i_{reduction}=i_{H_3O^+/H_2}+i_{HCO_3^-/CO_3^{2-}}+i_{H_2O/OH^-} \tag{20}$$

This expression can be written as:

$$\sum i_{red}=i_{0,H_3O^+/H_2}\times10^{(E-E_{rev,H_3O^+/H_2})/\beta_{H_3O^+/H_2}}+i_{0,HCO_3^-/CO_3^{2-}}\times10^{(E-E_{rev,HCO_3^-/CO_3^{2-}})/\beta_{HCO_3^-/CO_3^{2-}}}+i_{0,H_2O/OH^-}\times10^{(E-E_{rev,H_2O/OH^-})/\beta_{H_2O/OH^-}} \tag{21}$$

The reversible potential, E_{rev}, for each reaction was calculated using Nernst equation. In this case, the reversible potential for ferum oxidation reaction can be determined as follow:

$$E_{rev\,(Fe/Fe+2)} = E^0 + \frac{2.3RT}{nF}\log\frac{[Fe]}{[Fe^{2+}]} \quad (22)$$

where E^0 = Standard electrode potentials of ferum oxidation reaction

$[J]$ = Species Concentration

n = number of electrons involved in the reaction

F = Faraday Constant, 96500 coulombs/equivalent

The values for standard electrode potential for oxidation and reduction reactions are given in the following Table III.

TABLE III: STANDARD ELECTRODE POTENTIAL FOR OXIDATION & REDUCTION REACTION

Reaction	Standard electrode potential, E_0
Oxidation of Fe	0.447
Reduction of H_3O^+	0
Reduction of HCO_3^-	0.588
Reduction of H_2O	0.8277

The parameters exchange current density, i_0 and Tafel constants, β for each reaction at various pH conditions are shown in Table IV.

TABLE IV: TAFEL CONSTANT & EXCHANGE CURRENT DENSITY FOR OXIDATION-REDUCTION REACTION

Reaction	pH	Tafel constant, β, (mV/decade)	Exchange Current Density, i
Fe/Fe^{2+}	2.0	50	0.00002
	4.0	55	0.05
	6.2	70	0.046
	8.1	72	0.024
	10.0	124	0.47
H_2O/H_2	4.0	160	0.04
	6.2	160	0.2
	8.1	125	0.16
	10.0	78	0.25
H^+/H_2	2.0	100	3.8
	4.0	120	0.65
HCO_3^-/H_2	6.2	175	1.0
	8.1	160	4.6
	10.0	133	2.0

Other parameters such as mixed potential, E_{corr}, in various temperatures and CO_2 loadings, H_2O and Fe concentration in the system are presented in the following Tables V and VI.

TABLE V: MIXED POTENTIAL OF MODELED SYSTEM FROM EXPERIMENTAL DATA

Temperature °C	CO_2 Loading Mole/mole	Mixed Potential, E_{corr} (V)
40	0.1	-0.7843
	0.5	-0.7697
	1.0	-0.7657
60	0.1	-0.8074
	0.5	-0.8002
	1.0	-0.7945
80	0.1	-0.8572
	0.5	-0.8396
	1.0	-0.8163

TABLE VI: CONCENTRATION OF H_2O AND FE IN THIS SYSTEM (CONSTANT)

Species	Concentration, (mole/l)
H_2O	49.7
Fe	8.44×10^{-5}

IV. EXPERIMENTAL SET UP AND PROCEDURE

The experiments were conducted in a static corrosion cell using an electrochemical technique. The experimental setup as shown in Fig. 1 consists essentially of a corrosion cell, potentiostat /galvanostat and a radiometer. The corrosion cell contains a 250 mL flask, auxiliary electrode, reference electrode, and a working electrode. During each run a gas mixture of CO_2 and N_2 is bubbled through the cell until gas-liquid equilibrium is attained when a constant pH value of the solution is reached. Then, a potentio-dynamic technique is used to run the corrosion tests. In this procedure, before each polarization experiment the steel working electrode surface (specimen) was polished with 600 grit silicon carbide papers. Then mounted on the specimen holder (rotating working electrode), and immersed into the carbonated amine solution. The working electrode was subjected to a constant rotation speed of 600 rpm via a radiometer speed control unit. Platinum wire was used as counter electrode. Potential scanning was effected using a radiometer potentiostat /galvanostat connected to a PC dotted with a control and data acquisition system. The corrosion cell is maintained at the specified temperature, and CO_2 partial pressure. A continuous flow of the gas mixture at predetermined proportions was passed into the cell to ensure a constant amine loading in the solution

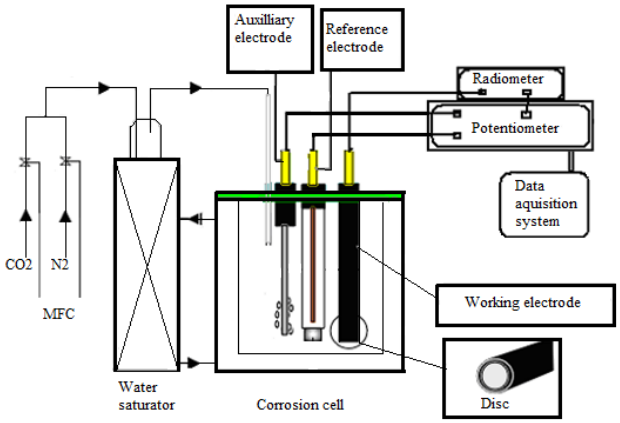

Fig. 1. Schematic diagram of the experimental set up.

V. MODELING APPROACH

A computer program based on the above mathematical model was developed to simulate the corrosion process in the DEA-CO_2-H_2O system. To execute the numerical simulation, input information, including total amine concentration, solution temperature, CO_2 loading, electrode potential and choice of oxidizing agents, was required. The model simulation began with determination of the physical properties and equilibrium constants for all chemical reactions (reactions 1–7) in Table I. An initial guess for the surface concentrations of all species was then made. The ionic strength was calculated and subsequently used to estimate the activity coefficients for the individual species. Then, a new equilibrium constant for all chemical reactions is determined using the new activity coefficients and concentration through equations (E1–E7). The equations (E1–E11) were resolved to get new chemical species concentrations.

A. Simulated Polarization Curves

Simulated anodic and cathodic polarization curves were estimated based on the calculated species concentrations. The

polarization curves were characterized by the following relationship

$$E - E_{rev} = \beta\left(\log\left(i/i_0\right)\right) \quad (24)$$

Any polarization curve begins at a coordinate (i_0, E_{rev}) and proceeds in the direction that the current density i increases with a slope of β. A simplified flow chart of simulation steps for corrosion model is presented in Fig. 2.

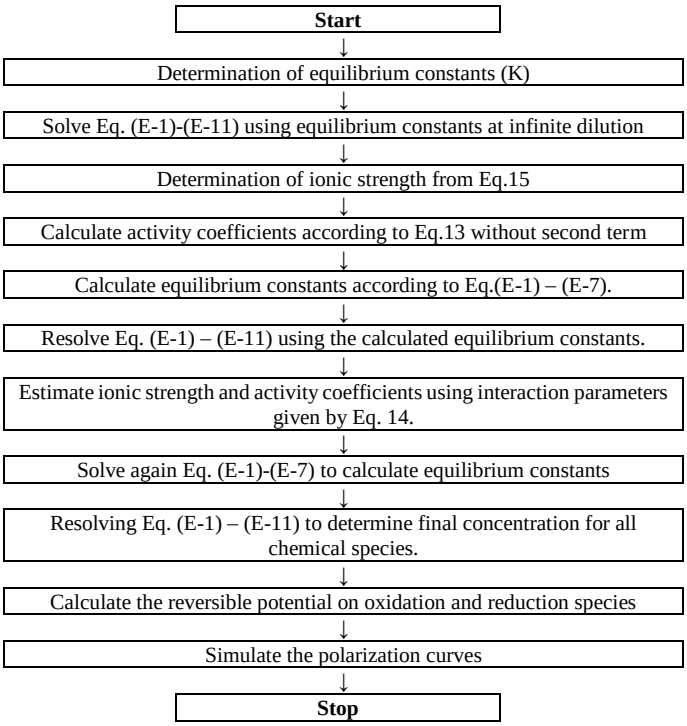

Fig. 2. Simplified flow chart of simulation steps for corrosion model.

VI. Results and Discussion

H_3O^+, HCO_3^- and H_2O are the potential oxidizing agents in an H_2O-DEA-CO_2 system. As listed in Table VII, these species lead to seven scenarios of possible oxidizing agents to be tested. For each test, the simulated polarization curve was plotted against the experimental curve as following the approach of [12]. The accepted scenario will be the one for which both anodic and cathodic branches of the simulated curves fit the experimental curves.

Fig. 2-Fig. 4 illustrate simulated and experimental curves obtained for a 2M DEA solution at 60 °C and 0.1 (mol/mol) CO_2 loading. In case of scenario 1, where H_3O^+ is the only considered oxidizing agent in the system (Fig. 3), there is a poor agreement between the simulated and experimental polarization curves. This indicates that H_3O^+ does not play a dominant role in the reduction reaction. As a result, it was necessary to further investigate the other scenarios.

The simulated curves based on the oxidizing agent H_2O is shown in Fig. 4. It has a similar orientation as the experimental curve especially with regard to the anodic branch. This implies that H_2O has a minor contribution to the reduction reaction. Nevertheless, this scenario is still not a complete representation of the actual corrosion behaviour and further analysis is required.

Fig. 5 presents the simulated polarization curves based on scenario 6 where H_2O and HCO_3^- are both oxidizing agent. The simulated curves match well with the experimental curves and gave a good indication of the system corrosion behaviour. This suggests that H_2O and HCO_3^- play a significant role in the corrosion process. Other scenarios for different combination of the oxidizing agents involve (H_3O+, HCO_3^-) and (H_3O^+, H_2O) as well as HCO_3^- with other scenarios showed no significant effect of these combinations in predicting the corrosion behaviour in the system. So, at this point, we can conclude that H_2O, HCO_3^- are the only oxidizing agent responsible for corrosion for the considered condition.

TABLE VII: Scenarios for Oxidizing Agent Identification

Scenario	Oxidizing Agent
1	H_3O^+
2	HCO_3^-
3	H_2O
4	H_3O^+ and HCO_3^+
5	H_3O^+ and H_2O
6	HCO_3^- and H_2O
7	H_3O^+, HCO_3^- and H_2O

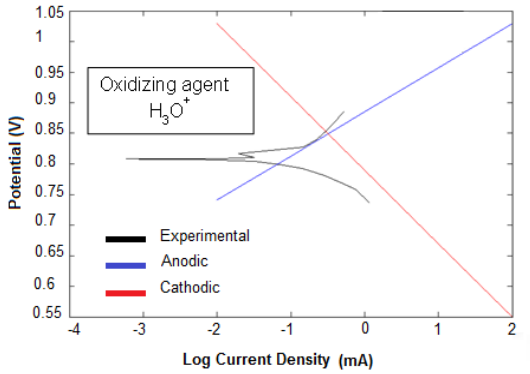

Fig. 3. Simulated and experimental curves for 2 M DEA solution at 60 °C and 0.1 CO_2 loading.

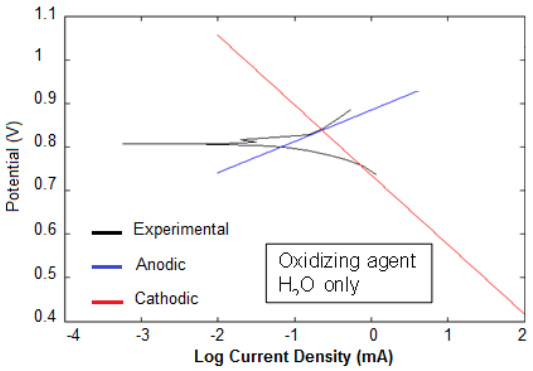

Fig. 4. Simulated and experimental curves for 2 M DEA solution at 60 °C and 0.1CO_2 loading.

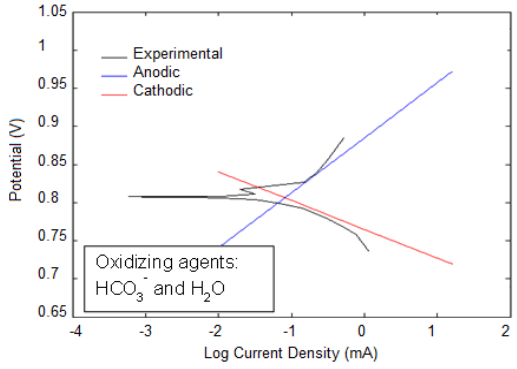

Fig. 5. Simulated and experimental curves for 2 M DEA solution at 60°C and 0.1 CO_2 loading.

VII. Conclusion

A mechanistic corrosion model was developed using a rigorous equilibrium model based on an activity coefficient approach according to Debye-Huckel theory and mixed potential theory. This model was used to identify the oxidizing agents responsible for corrosion in an aqueous DEA-CO_2 environment. Polarization curves of the chemical species at a metal-solution interface were successfully simulated. It was found that H_2O and HCO_3^- are the main oxidizing agents at a temperature 60°C.

References

[1] J. D. Harston and F. Ropital, *Amine Unit Corrosion in Refineries, European Federation of Corrosion 46: Technical Background*, Woodhead Publishing and Maney Publishing, The Institute of Materials, Minerals & Mining, Boca Raton Boston New York Washington, DC: CRC Press, 2007.

[2] A. L. Kohl and R. B. Nielsen, *Gas Purification*, 5th ed., Gulf Publishing Company, Texas, USA, 1997.

[3] American Petroleum Institute, *Corrosion of Oil-and Gas-Well Equipment*, API, Dallas, Texas, 1958.

[4] S. Nesic, J. Postlethwaite, and M. Vrhovac, *Corrosion Reviews*, vol. 15, no. 2, pp. 211-240, 1997.

[5] M. S. DuPart, T. R. Bacon, and D. J. Edwards, *Understanding corrosion in alkanolamine gas treating plants, Part2. Case histories show actual plant problems and their solutions*, Hydrocarbon Process, pp. 75-80, 1993.

[6] S. Teeradet, I. Raphael, T. Paitoon, and S. Chintana, "Kinetics of sulphur dioxide- and oxygen-induced degradation of aqueous monoethanolamine solution during CO_2 absorption from power plant flue gas streams," *Journal of Greenhouse Gas Control*, vol. 3, pp. 133-142, 2009.

[7] L. M. Galan, G. W. Meindersma, and A. B. de-Haan, *Basic Data, Eva Sorensen, Distillation & Absorption Symposium Series No. 152*, UK: Institution of Chemical Engineers (IChemE), pp. 511-522, 2006.

[8] P. Pearson, A. F. Hollenkamp, and E. Meuleman, "Electrochemical investigation of corrosion in CO_2 capture plants—influence of amines," *Electrochimica Acta*, vol. 110, pp. 511– 516, 2013.

[9] B. Zhao, Y. Sun, Y. Yuan, J. Gao, S. Wang, Y. Zhuo, and C. Chen., "Study on corrosion in CO_2 chemical absorption process using amine solution," *Energy Procedia*, vol. 4, pp. 93–100, 2011.

[10] P. Wattanaphana, T. Semaa, R. Idem, Z. Lianga, and P. Tontiwachwuthikul, "Effects of flue gas composition on carbon steel (1020) corrosion in MEA-based CO_2 capture process," *International Journal of Greenhouse Gas Control*, vol. 19, pp. 340–349, 2013.

[11] B. Richard, *An Introduction to Corrosion: A general introduction to the processes of corrosion and methods to reduce its effects*, ch. 2, 2004.

[12] A. Veawab and A. Aroonwilas, "Identification of oxidizing agents in aqueous amine-CO_2 systems using a mechanistic corrosion model," *Corrosion Science*, vol. 44, 2002.

[13] A. Dugstad, L. Lunde and K. Videm, "Parametric study of CO_2 corrosion of carbon steel," *Corrosion*, vol. 94, pp. 14, 1994.

[14] W. P. Jepson, C. Kang, M. Gopal, and S. Stitzel, "Model sweet corrosion in horizontal multiphase slug flow," *Corrosion*, vol. 97, pp. 11, 1997.

[15] A. M. K. Halvorsen and T. Sontvedt, "CO_2 corrosion model for carbon steel including a wall shear stress model for multiphase flow and limits for production rate to avoid mesa attack," *Corrosion*, vol. 99, pp. 42, 1999.

[16] M. Nordsveen, S. Nesic, R. Nyborg, and A. Stangeland, "A mechanistic model for carbon dioxide corrosion of mild steel in the presence of protective iron carbonate films-Part1: Theory and Verification," *Corrosion*, vol. 59, no. 5, pp. 443, 2003.

[17] G. N. Lewis, M. Randall, K. S. Pitzer, and L. Brewer, *Thermodynamics*, second ed., McGraw Hill, 1961.

[18] K. S. Pitzer, "Thermodynamics of electrolytes. I. theoretical basis and general equations," *J. Phys. Chem.*, vol. 77, issue 2, pp. 268–277, 1973.

[19] K. S. Pitzer and J. J. Kim, *J. Am. Chem. Soc.*, vol. 96, pp. 5701–5707, 1974.

[20] Benamor and M. K. Aroua, "Modelling of CO_2 solubility and carbamate concentration in DEA, MDEA and their mixtures using Deshmukh-Mather model," *Fluid Phase Equilibria*, 2005.

[21] I. M. Klotz and R. M. Rosenberg, *Chemical Thermodynamics: Basis Theory and Methods*, 5th ed., Wiley, New York, 1994.

[22] D. A. Jones, *Principles and Prevention of Corrosion*, Macmillan, New York, 1992.

Abdelbaki Benamor was born in Algeria in 1967. He obtained his "Ingenieur d'Etat" degree in Chemical Process Engineering from the University of Bejaia (Algeria) in 1994. After a two years period in the private sector industry, he obtained his MSc from the University of Malaya (Malaysia) in 1998 and PhD in 2003 from the same university.

He has more than ten years' experience in academic and research. He is currently working as an assistant research professor at the Gas Processing Center, Qatar University. His work is essentially related to all aspects of carbon capture from natural gas and flue gases. His has a special interest in process systems analysis and design. In 2003, he joined the Department of Chemical Engineering, University of Malaya as a lecturer. In 2005, he moved to the University of Nottingham as assistant professor until 2009. Before joining Qatar University in October 2011, he was attached with Sohar University, Oman.